

# An Interval-Based Bayesian Generative Model for Human Complex Activity Recognition

Li Liu<sup>1,2,3</sup>, *Member, IEEE* Yongzhong Yang<sup>4</sup>, Lakshmi N. Govindarajan<sup>4</sup>, Shu Wang<sup>5</sup>,

Bin Hu<sup>6</sup>, *Senior Member, IEEE* Li Cheng<sup>3,4</sup>, *Senior Member, IEEE*, and David S. Rosenblum<sup>3</sup>, *Fellow, IEEE*

<sup>1</sup>Ministry of Education, Key Laboratory of Dependable Service Computing in Cyber Physical Society, Chongqing 400044, China

<sup>2</sup>School of Software Engineering, Chongqing University, Chongqing 400044, China

<sup>3</sup>School of Computing, National University of Singapore, 117417, Singapore

<sup>4</sup>Bioinformatics Institute, A\*STAR, 138671, Singapore

<sup>5</sup>College of Material Science and Engineering, Lanzhou University of Technology, Lanzhou 730050, China

<sup>6</sup>School of Information Science and Engineering, Lanzhou University, 730000, China

Complex activity recognition is challenging due to the inherent uncertainty and diversity of performing a complex activity. Normally, each instance of a complex activity has its own configuration of atomic actions and their temporal dependencies. We propose in this paper an atomic action-based Bayesian model that constructs Allen's interval relation networks to characterize complex activities with structural varieties in a probabilistic generative way: By introducing latent variables from the Chinese restaurant process, our approach is able to capture all possible styles of a particular complex activity as a unique set of distributions over atomic actions and relations. We also show that local temporal dependencies can be retained and are globally consistent in the resulting interval network. Moreover, network structure can be learned from empirical data. A new dataset of complex hand activities has been constructed and made publicly available, which is much larger in size than any existing datasets. Empirical evaluations on benchmark datasets as well as our in-house dataset demonstrate the competitiveness of our approach.

*Index Terms*—complex activity recognition, Allen's interval relation, Bayesian network, probabilistic generative model, Chinese restaurant process, temporal consistency, American Sign Language dataset.

## I. INTRODUCTION

A *complex activity* consists of a set of temporally-composed events of *atomic actions*, which are the lowest-level events that can be directly detected from sensors. In other words, a complex activity is usually composed of multiple atomic actions occurring consecutively and concurrently over a duration of time. Modeling and recognizing complex activities remains an open research question as it faces several challenges: First, understanding complex activities calls for not only the inference of atomic actions, but also the interpretation of their rich temporal dependencies. Second, individuals often possess diverse styles of performing the same complex activity. As a result, a complex activity recognition model should be capable of capturing and propagating the underlying uncertainties over atomic actions and their temporal relationships. Third, a complex activity recognition model should also tolerate errors introduced from atomic action level, due to sensor noise or low-level prediction errors.

### A. Related Work

Currently, a lot of research focuses on semantic-based complex activity modeling. Many semantic-based models such as context-free grammar (CFG) [26] and Markov logic network (MLN) [11], [18]) are used to represent complex activities, which can handle rich temporal relations. Yet formulae and their weights in these models (e.g. CFG grammars and MLN structures) need to be manually encoded, which could be rather difficult to scale up and is almost impossible for many

practical scenarios where temporal relations among activities are intricate. Although a number of semantic-based approaches have been proposed for learning temporal relations, such as stochastic context-free grammars [29] and Inductive Logic Programming (ILP) [9], they can only learn formulas that are either true or false, but cannot learn their weights, which hinders them from handling uncertainty.

On the other hand, graphical models become increasingly popular for modeling complex activities because of their capability of managing uncertainties [31]. Unfortunately, most of them can handle three temporal relations only, i.e. equals, follows and precedes. Both Hidden Markov model (HMM) and conditional random field (CRF) are commonly used for recognizing sequential activities, but are limited in managing overlapping activities [13]. Many variants with complex structures have been proposed to capture more temporal relations among activities, such as interleaved hidden Markov models (IHMM) [20], skip-chain CRF [12] and so on. However, these models are time point-based, and hence with the growth of the number of concurrent activities they are highly computationally intensive [22]. Dynamic Bayesian network (DBN) can learn more temporal dependencies than HMM and CRF by adding activities' duration states, but imposes more computational burden [21]. Moreover, the structures of these graphical models are usually manually specified instead of learned from the data. The interval temporal Bayesian network (ITBN) [31] differs significantly from the previous methods, as being a graphical model that first integrates interval-based Bayesian network with the 13 Allen's relations. Nonetheless, ITBN

has several significant drawbacks: First, its directed acyclic Bayesian structure makes it have to ignore some temporal relations to ensure a temporally consistent network. As such, it may result in loss of internal relations. Second, it would be rather computationally expensive to evaluate all possible consistent network structures, especially when the network size is large. Third, neither can ITBN manage the multiple occurrences of the same atomic action, nor can it handle arbitrary network size as it remains unchanged as the count of atomic action types. Figure 1 illustrates the graph structures of the three commonly-used graphical models. It is worth

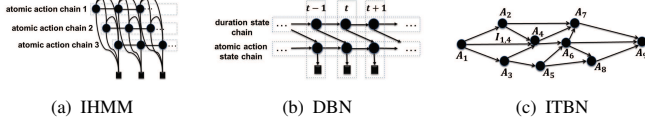


Figure 1. The structures of three graphical models for complex activity recognition. (a) IHMM, where the observations of atomic actions (square-shaped nodes) and several chains of hidden states (round-shaped nodes) are used to handle overlapping; (b) DBN, where duration states and atomic action states are represented as chains of nodes; (c) ITBN, where any atomic action type ( $A_1$ - $A_9$ ) is represented by a node and the set of all possible interval relations between any pair of atomic action types  $A_i$  and  $A_j$  is represented by a link  $I_{i,j}$ .

noting that we will focus on complex activity recognition in this paper, and interested readers may consult the excellent reviews [1], [6], [14], [7], [4], [8] for further details regarding atomic-level action recognition.

### B. Our approach

To address the problems in the previous models, we present an *interval-based Bayesian generative network* (IBGN) to explicitly model complex activities with inherent structural varieties, which is achieved by constructing probabilistic interval-based networks with temporal dependencies. In other words, our model considers a probabilistic generative process of constructing interval-based networks to characterize the complex activities of interests. Briefly speaking, a set of latent variables, called *tables*, which are generated from the *Chinese restaurant process* (CRP) [23] are introduced to construct the interval-based network structures of a complex activity. Each latent variable characterizes a unique *style* of this complex activity by containing its distinct set of atomic actions and their temporal dependencies based on Allen’s interval relations. There are two advantages to using CRP: It allows our model to describe a complex activity of arbitrary interval sizes and also to take into account multiple occurrences of the same atomic actions. We further introduce *interval relation constraints* that can guarantee the whole network generation process is globally temporally consistent without loss of internal relations. In addition, instead of manually specify a network to a fixed structure, the network structure in our approach is learned from training data. By *learning network structures*, our model is more effective than existing graphical models in characterizing the inherent structural variability in complex activities. A further comparison study is summarized in Table I, which also shows our main contributions.

Table I  
A SUMMARY COMPARISON OF GRAPHICAL MODEL-BASED APPROACHES FOR RECOGNIZING COMPLEX ACTIVITIES.

	HMMs & BNs	ITBN	our IBGN
Time-point-based (p) or interval-based (i)?	p	i	i
How many temporal relations can be described?	3	13	13
Retain all the interval relations during training stage?	✓	X	✓
Handle any possible combinations of interval relations?	X	✓	✓
Handle multiple occurrences of the same atomic action?	✓	X	✓
Handle variable number of overlapping actions?	X	✓	✓
Describe a complex activity with variable sizes of points or intervals?	✓	X	✓
Is the structure learned from training data?	X	✓	✓

It is worth mentioning that in spite of the increasing need from diverse applications in the area of complex activity recognition, there are only a few publicly-available complex activity recognition datasets [25], [3], [15]. In particular, the number of instances are on the order of hundreds at most. This motivates us to propose a dedicated large-scale dataset on depth camera-based complex hand activity recognition. We have constructed a new dataset of complex hand activities which contains instances that are about an order of magnitude larger than the existing datasets. We have made the dataset and related tools made publicly available on a dedicated project website<sup>1</sup> in support of the open-source research activities in this emerging research community.

## II. DEFINITIONS AND PROBLEM FORMULATION

Assume we have at hand a dataset  $\mathbb{D}$  of  $N$  instances from a set of  $L$  types of complex activities involving a set of  $M$  types of atomic actions  $\mathbb{A} = \{A_1, A_2, \dots, A_M\}$ . An *atomic action interval* (*interval* for short) is written by  $I_i = a_i @ [t_i^-, t_i^+]$ , where  $t_i^-$  and  $t_i^+$  represent the start and end time of the atomic action  $a_i \in \mathbb{A}$ , respectively. Each complex activity instance is a sequence of  $k$  ordered intervals, i.e.  $\langle I_1, I_2, \dots, I_k \rangle$ , such that if  $1 \leq i < j \leq k$ , then  $(t_i^- < t_j^-)$  or  $(t_i^- = t_j^- \text{ and } t_i^+ \leq t_j^+)$ . Seven Allen’s interval relations (*relations* for short) [2] are used to represent all possible temporal relationships between two intervals, denoted by  $\mathbb{R} = \{b, m, o, s, c, f, \equiv\}$ , which is summarized below:

$$\begin{aligned}
 (\text{before}) \quad I_i \ b \ I_j &: t_i^+ < t_j^-, \\
 (\text{meet}) \quad I_i \ m \ I_j &: t_i^+ = t_j^-, \\
 (\text{overlap}) \quad I_i \ o \ I_j &: t_i^- < t_j^- < t_i^+ < t_j^+, \\
 (\text{start}) \quad I_i \ s \ I_j &: t_i^- = t_j^- \text{ and } t_i^+ < t_j^+, \\
 (\text{contain}) \quad I_i \ c \ I_j &: t_i^- < t_j^- \text{ and } t_i^+ < t_j^+, \\
 (\text{finished-by}) \quad I_i \ f \ I_j &: t_i^- < t_j^- \text{ and } t_i^+ = t_j^+, \\
 (\text{equal}) \quad I_i \ \equiv \ I_j &: t_i^- = t_j^- \text{ and } t_i^+ = t_j^+.
 \end{aligned}$$

We define an interval-based network (*network* for short)  $G = (V, E)$  to represent a complex activity containing the temporal relationships between intervals. A node  $v_i \in V$  represents the  $i$ -th interval (i.e.  $I_i$ ) in a complex activity instance, while a directed link  $e_{i,j} \in E$  represents the relation between two intervals (i.e.  $I_i$  and  $I_j$ ), where  $1 \leq i < j \leq |V|$  ( $|V|$  is the cardinality of the set  $V$ ). Note a link always starts from a node with a smaller index than its arrival node. Each link  $e_{i,j}$

<sup>1</sup>The dataset including raw videos, annotations and related tools can be found at <http://web.bii.a-star.edu.sg/~lakshming/complexAct/>.

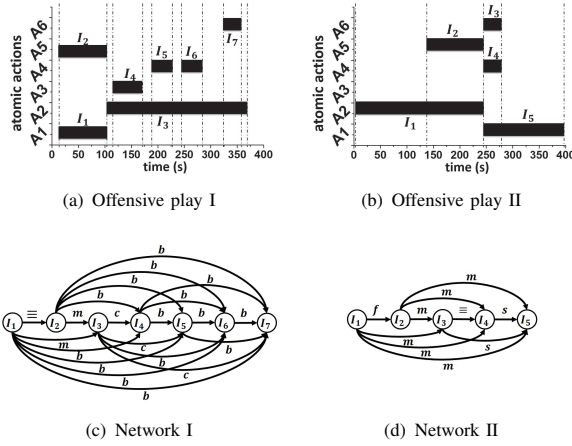


Figure 2. Two possible styles of the complex activity *offensive play* and its corresponding networks where the nodes represent the intervals of atomic actions and the links represent their temporal relations. Atomic actions:  $A_1 = \text{walk}$ ,  $A_2 = \text{stand}$ ,  $A_3 = \text{hold ball}$ ,  $A_4 = \text{jump}$ ,  $A_5 = \text{dribble}$ ,  $A_6 = \text{shoot}$ .

involves one and only one relation  $r_{i,j} \in \mathbb{R}$ . Figure 2 illustrates the corresponding networks of a complex activity.

The temporal relations on links shall be globally consistent in any interval-based network. Given any two relations  $r_{i,j}, r_{j,k} \in \mathbb{R}$  on links  $e_{i,j}$  and  $e_{j,k}$ , respectively, the relation  $r_{i,k}$  on link  $e_{i,k}$  must follow the transitivity properties as shown in Figure 3. For example, suppose  $I_i$  meets  $I_j$  and  $I_j$  starts  $I_k$ ,  $I_i$  is certainly meets  $I_k$ . However, if  $I_i$  starts  $I_j$  and  $I_j$  is finished by  $I_k$ , there are three possible relations between  $I_i$  and  $I_k$ , that is, before, meet and overlap. We formally use  $r_{i,j} \circ r_{j,k}$  to denote such *composition* operation following the transitivity properties. We say a network is *consistent* such that  $r_{i,k} \in r_{i,j} \circ r_{j,k}$  for any triplet of links  $e_{i,j}$ ,  $e_{j,k}$  and  $e_{i,k}$  in the network.

$r_{i,j} \circ r_{j,k}$	$b$	$m$	$o$	$s$	$c$	$f$	$\equiv$
$b$	$b$	$b$	$b$	$b$	$b$	$b$	$b$
$m$	$b$	$b$	$b$	$m$	$b$	$b$	$m$
$o$	$b$	$b$	$bmo$	$o$	$bmocf$	$bmo$	$o$
$s$	$b$	$b$	$bmo$	$s$	$bmocf$	$bmo$	$s$
$c$	$bmocf$	$ocf$	$ocf$	$ocf$	$c$	$c$	$c$
$f$	$b$	$m$	$o$	$o$	$c$	$f$	$f$
$\equiv$	$b$	$m$	$o$	$s$	$c$	$f$	$\equiv$

Figure 3. The transitivity table for any interval relation  $r_{i,k}$  through composition operation  $r_{i,j} \circ r_{j,k}$ .

It is clear that a network can characterize one possible style of a complex activity with diverse combinations of atomic actions and their interval relations, as illustrated in Figure 2. From another point of view, a complex activity can be instantiated by sampling atomic actions and relations assigned to their associated nodes and links in a network following certain probabilities. In this way, a recognition model built on such networks is able to handle uncertainty in complex activity recognition. In addition, multiple occurrences of the same atomic action can appear in the same network but in different nodes (i.e. intervals). To this end, we present the probabilistic generative model IBGN where these networks

can be constructed following the styles of the complex activities of interests under uncertainty. We shall also consider the IBGN model to construct networks with variable sizes of nodes and arbitrary structures. Note in our approach, for each type of complex activities we would learn one such dedicated IBGN model.

### III. OUR IBGN MODEL

For any complex activity type  $l$  ( $1 \leq l \leq L$ ), denote  $\mathbb{D}_l \subseteq \mathbb{D}$  the corresponding subset of  $N_l$  instances, where each element  $d \in \mathbb{D}_l$  is an instance of the  $l$ -th type of complex activity. In IBGN, the generative process of constructing an interval-based network  $G_d = (V_d, E_d)$  for describing the observed instance  $d$  consists of two parts, node generation and link generation, which are described below.

#### A. Node Generation

In our IBGN model, we consider generating a network where each node is associated with an atomic action in a probabilistic manner. We also require our model to be capable of generating variable numbers of nodes and handling multiple occurrences of the same atomic action in our network, as summarized in Table I.

To accomplish these tasks, we first extend the process of the CRPs to make it available in our IBGN model. Originally, a CRP is analogous to a stochastic process of choosing tables for customers in a Chinese restaurant. In a nutshell, suppose there are an infinite number of tables  $\{T_1, T_2, \dots\}$ . The first customer ( $n = 1$ ) always selects the first table; Any other customer ( $n > 1$ ) randomly selects an occupied table or an unoccupied empty table with a certain probability.

We continue this process by serving dishes right after each customer is seated at a table. Assume there are a finite number of dishes and an infinite number of cuisines. Each table is associated with a cuisine that dishes are served with a unique probability distribution. Any customer sitting at a table randomly selects a dish with the probability relating to its corresponding cuisine.

In our model, a network contains a group of customers where each customer is analogous to a node while a dish is analogous to an atomic action type. Suppose customers from the same group prefer similar cuisines, which is analogous to a complex activity of interest, and are more likely to sit at the same tables. Formally, denote  $\{\mathbf{t}_1, \mathbf{t}_2, \dots\}$  the variables of tables, and  $\{\mathbf{a}_1, \mathbf{a}_2, \dots\}$  the variables of atomic actions<sup>2</sup>. To construct a network  $G_d = (V_d, E_d)$ ,  $\mathbf{t}_n$  and  $\mathbf{a}_n$  are the table and the atomic action (dish) assigned to the node (customer)  $v_n \in V_d$  ( $n = 1, 2, \dots, |V_d|$ ). The generative process operates as follows. The  $n$ -th node  $v_n$  selects a table  $\mathbf{t}_n$  that is drawn from the following distribution:

$$P(\mathbf{t}_n = T_\zeta | \mathbf{t}_1, \dots, \mathbf{t}_{n-1}) = \begin{cases} \frac{m_\zeta}{n + \alpha - 1} & \text{if } T_\zeta \text{ is a non-empty table,} \\ \frac{\alpha}{n + \alpha - 1} & \text{if } T_\zeta \text{ is a new table,} \end{cases} \quad (1)$$

<sup>2</sup>Whenever possible, we would use bold lowercase letters such as  $\mathbf{t}_n$ ,  $\mathbf{a}_n$  to represent variables, and uppercase letters such as  $T_i$  and  $A_j$  to represent generic values of these variables.

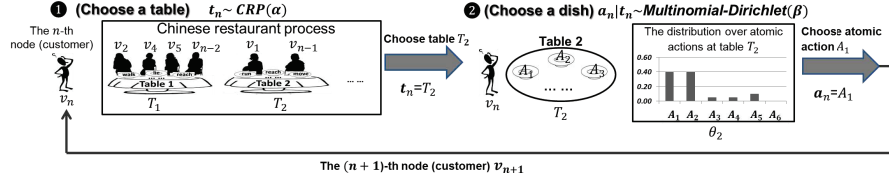


Figure 4. An illustration of the generative process of choosing a table  $t_n$  and an atomic action  $a_n$  for node  $v_n$ .

where  $nt_\zeta$  is the number of existing nodes occupied at table  $T_\zeta$  ( $\zeta = 1, 2, \dots$ ), with  $\sum_\zeta nt_\zeta = n - 1$ ,  $\mathbf{t} = T_1$ .  $\alpha$  is a tuning hyperparameter. It is worth mentioning that the distribution over table assignments in *CRP* is invariant and exchangeable under permutation according to de Finetti's Theorem [28]. After  $v_n$  is assigned with a table  $t_n = T_\zeta$ , an atomic action (dish)  $a_n$  is chosen from the table by:

$$(\mathbf{a}_n | t_n) \sim \text{Multinomial}(\theta_\zeta),$$

$$\theta_\zeta \sim \text{Dirichlet}(\beta),$$

where  $\beta$  is a hyperparameter. Note  $\theta_\zeta = (\theta_{\zeta,1}, \dots, \theta_{\zeta,M})^T$  is the parameter vector of a multinomial distribution at table  $T_\zeta$ . Figure 4 presents a cartoon explanation of this node generation process of our IBGN model. Since we would obtain one

relation  $\mathbf{r}_{n',n}$  on link  $e_{n',n}$  shall follow the transitivity properties listed in Figure 3. It is straightforward to verify that the set  $\mathbb{R}$  is closed under the composition operation. As a result, by applying the transitivity table, for any composition there exists only 11 possible transitive relations in Figure 6, denoted as  $\mathbb{C} = \{C_z : 1 \leq z \leq 11\}$ . In other words, any composition of two consecutive relations satisfies  $\mathbf{r}_{n',n''} \circ \mathbf{r}_{n'',n} \in \mathbb{C}$ .

$$\begin{aligned} C_1 &= \{b\}, C_2 = \{m\}, C_3 = \{o\}, C_4 = \{s\}, C_5 = \{c\}, C_6 = \{f\}, C_7 = \{\equiv\}, \\ C_8 &= \{b, m, o\}, C_9 = \{o, c, f\}, C_{10} = \{b, m, o, c, f\}, C_{11} = \{b, m, o, s, c, f, \equiv\}. \end{aligned}$$

Figure 6. The 11 possible interval composition relations.

To construct a *globally consistent network*, the relations on every triangle in a network must also be consistent. Namely, for any triplet of nodes  $v_{n'}$ ,  $v_{n''}$  and  $v_n$ , if there exist three links  $\mathbf{r}_{n',n}$ ,  $\mathbf{r}_{n',n''}$ , and  $\mathbf{r}_{n'',n}$ , they need to satisfy the transitive relation  $\mathbf{r}_{n',n} \in \mathbf{r}_{n',n''} \circ \mathbf{r}_{n'',n}$ . As such, we define the *interval relation constraint* variable as follows:

**Definition 1.** Give an arbitrary interval-based network  $G = (V, E)$ , the interval relation constraint  $\mathbf{c}_{n',n} \in \mathbb{C}$  for a link  $e_{n',n} \in E$  ( $1 \leq n' < n \leq |V|$ ) is

$$\mathbf{c}_{n',n} = \begin{cases} \bigcap_{n''=n'+1}^{n-1} (\mathbf{x}_{n',n''} \circ \mathbf{x}_{n'',n}) & \text{if } n > n' + 1, \\ \mathbb{R} & \text{if } n = n' + 1, \end{cases}$$

$$\text{where } \mathbf{x}_{p,q} = \begin{cases} \mathbf{r}_{p,q} & \text{if } e_{p,q} \in E, \\ \mathbf{c}_{p,q} & \text{if } e_{p,q} \notin E, \end{cases} \quad (n' \leq p < q \leq n).$$

In link generation, our IBGN model follows the rule that any relation  $\mathbf{r}_{n',n}$  can only be drawn from  $\mathbf{c}_{n',n}$ . We have proved that a network constructed under this rule is globally consistent and complete, with proofs relegated to the Appendix A.

**Theorem 1. (Network Consistency and Completeness)**

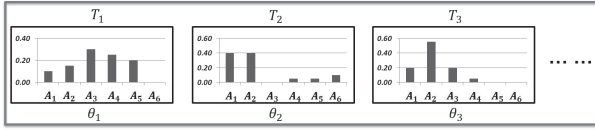
A network  $G_d$  constructed by obeying the interval relation constraints is always temporally consistent, and any possible combination of relations in  $G_d$  can be constructed through our IBGN model.

Now, we are ready to assign relations to links. Suppose  $\mathbf{a}_{n'} = A_i$ ,  $\mathbf{a}_n = A_j$  and  $\mathbf{c}_{n',n} = C_z$  ( $1 \leq i, j \leq M$ ,  $1 \leq z \leq 11$ ), a relation  $\mathbf{r}_{n',n}$  on link  $e_{n',n} \in E_d$  is chosen from a distribution over all possible relations in  $\mathbf{c}_{n',n}$  as follows:

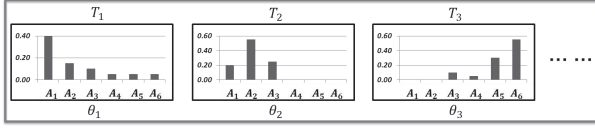
$$\mathbf{r}_{n',n} | \mathbf{a}_{n'}, \mathbf{a}_n, \mathbf{c}_{n',n} \sim \text{Multinomial}(\phi_{i,j,z}),$$

where  $\phi_{i,j,z}$  is the parameter vector of the multinomial distribution associated with the triplet  $(A_i, A_j, C_z)$ . Note that for an interval relation constraint containing only one relation (i.e.  $C_1$ - $C_7$ ), the probability of choosing that relation is always one.

It is also important to notice that the quality of the network structure plays an extremely important role in activity



(a) Distributions of atomic actions at different tables that collectively represent the complex activity *offensive play*.



(b) Distributions of atomic actions at different tables that collectively represent the complex activity *defensive play*.

Figure 5. Examples of the tables and corresponding distributions over atomic actions for representing two complex activities, *offensive play* and *defensive play*, respectively. Here each table contains a set of atomic actions under a specific distribution.

dedicated IBGN model for each complex activity, a complex activity is now characterized as a unique set of distributions over atomic actions, i.e.  $\theta = \{\theta_1, \theta_2, \dots\}$ . As illustrated in Figure 5, the two different complex activities *offensive play* and *defensive play* are associated with two distinct sets of tables with their own distributions over atomic actions. It suggests that our IBGN modeling approach is capable of differentiating the underlying characteristics associated with atomic actions from different complex activity categories.

## B. Link Generation

Once each node (interval) is assigned to an atomic action, links and their associated relations are to be generated next. It is important to ensure *consistency* of the resulting relations over all links. Formally, given two relations  $\mathbf{r}_{n',n''}$  and  $\mathbf{r}_{n'',n}$  on the links  $e_{n',n''}$  and  $e_{n'',n}$  ( $n' < n'' < n$ ), respectively, the interval

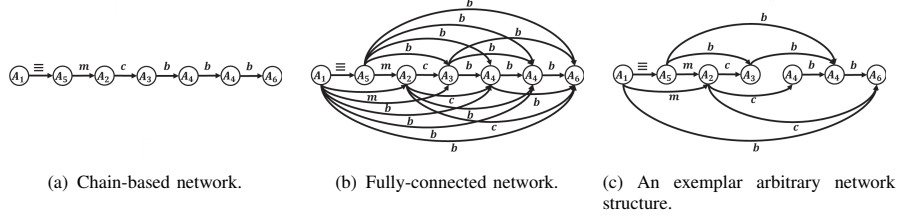


Figure 7. Three possible network structures in link generation.

modeling. In our previous work [17], two variants with fixed network structures are considered: *chain-based network* as in Figure 7(a), where only the links between two neighbouring nodes are constructed in networks; *fully-connected network* as in Figure 7(b), where all pairwise links are constructed in networks. In fact, they are two special cases of our IBGN model. In chain-based networks, only a set of  $|V_d| - 1$  links  $e_{1,2}, e_{2,3}, \dots, e_{|V_d|-1, |V_d|}$  are generated, with  $e_{n,n+1}$  ( $1 \leq n \leq |V_d| - 1$ ) representing the link of two neighboring nodes  $v_n \rightarrow v_{n+1}$ . Any interval relation constraint  $c_{n,n+1}$  in chain-based networks equals to  $\mathbb{R}$ , and thus such networks are inherently consistent because no inconsistent triangle exists. However crucial relations may be missing in this model. On the other side of the spectrum, we have fully-connected networks, where all possible pairwise links are considered. Any  $\mathbf{x}_{p,q}$  in fully-connected networks equals to  $\mathbf{r}_{p,q}$ . When fitting the IBGN model, it is possible to increase the likelihood by adding links, but doing so may result in overfitting. Instead of prefixing the network structures, in this work we relax the assumption of a structure being either fully-connected or chain-based, and consider learning an optimal structure (i.e. to decide which links should exist in the network) from data. This allows the IBGN model to handle temporal consistency for arbitrary network structures, as presented in Figure 7(c).

### C. The Generative Process

For each dataset  $\mathbb{D}_l \subset \mathbb{D}$  containing a particular complex activity  $1 \leq l \leq L$ , our model assumes the whole generative process including node generation and link generation in Algorithm 1. Notice that the optimal network structure  $\mathbf{G}^*$  would be learned from  $\mathbb{D}_l$  with details to be elaborated in section IV-A. The structure  $\mathbf{G}^*$  demonstrates whether a link needs to be generated in the network. For example, to construct the network  $G_d = (V_d, E_d)$  for a certain complex activity instance  $d$ , the link  $e_{n',n}$  from  $v_{n'}$  to  $v_n$  is involved in  $G_d$  if and only if  $e_{n',n}$  obeys the structure of  $\mathbf{G}^*$ , denoted by  $e_{n',n} \in E_d \models \mathbf{G}^*$ .

The joint distribution of variables  $\mathbf{t}$ ,  $\mathbf{a}$ , and  $\mathbf{r}$ , is given by:

$$P(\mathbf{a}, \mathbf{t}, \mathbf{r}; \alpha, \beta) = \prod_{d \in \mathbb{D}_l} \left( \prod_{v_n \in V_d} (P(\mathbf{t}_n | \mathbf{t}_1, \dots, \mathbf{t}_{n-1}; \alpha) P(\mathbf{a}_n | \mathbf{t}_n; \beta)) \prod_{\substack{n' < n, \\ e_{n',n} \models \mathbf{G}^*}} P(\mathbf{r}_{n',n} | \mathbf{a}_n, \mathbf{a}_{n'}, \mathbf{c}_{n',n}) \right). \quad (2)$$

The total number of variables  $\mathbf{t}$ ,  $\mathbf{a}$ , and  $\mathbf{r}$  are  $\sum_{d \in \mathbb{D}_l} |V_d|$ ,  $\sum_{d \in \mathbb{D}_l} |V_d|$  and  $|\mathbb{D}_l| \cdot |E_{\mathbf{G}^*}|$ , respectively. It is worth noting that

### Algorithm 1 Generative process.

---

```

1: procedure GENERATE-NETWORKS( $\mathbb{D}_l$ )
2:   Learn an optimal network structure  $\mathbf{G}^*$  from  $\mathbb{D}_l$ ;  $\triangleright \mathbf{G}^* = (V_{\mathbf{G}^*}, E_{\mathbf{G}^*})$ ,
3:   Choose a distribution  $\theta_\zeta \sim \text{Dirichlet}(\beta)$  ( $\zeta = 1, 2, \dots$ );
4:   for each complex activity instance  $d$  in  $\mathbb{D}_l$  do  $\triangleright$  construct a network
      $G_d = (V_d, E_d)$ 
5:     for each node  $v_n$  ( $1 \leq n \leq |V_d|$ ) do
6:       Choose a table  $\mathbf{t}_n \sim \text{CRP}(\mathbf{t}_1, \dots, \mathbf{t}_{n-1}; \alpha)$ ;  $\triangleright$  Suppose  $\mathbf{t}_n = T_\zeta$ 
7:       Choose an atomic action  $\mathbf{a}_n | \mathbf{t}_n \sim \text{Multinomial}(\theta_\zeta)$ ;  $\triangleright$  Suppose  $\mathbf{a}_n = A_j$ 
8:       for each link  $e_{n',n}$  ( $n-1 \geq n' \geq 1$ ) do
9:         if  $e_{n',n}$  obeys the structure of  $\mathbf{G}^*$  (i.e.  $e_{n',n} \models \mathbf{G}^*$ ) then
10:          Calculate  $\mathbf{c}_{n',n}$  on the link  $e_{n',n}$ ;  $\triangleright$  Suppose  $\mathbf{c}_{n',n} = C_\zeta$ 
11:          Choose a relation  $\mathbf{r}_{n',n} | \mathbf{a}_{n'}, \mathbf{a}_n, \mathbf{c}_{n',n} \sim \text{Multinomial}(\phi_{i,j,z})$ ;  $\triangleright$ 
            Suppose  $\mathbf{a}_{n'} = A_i$ 
12:          end if
13:        end for
14:      end for
15:    end for
16:  end procedure

```

---

we often set  $\ell = \max_{d \in \mathbb{D}_l} \{|V_d|\}$ , due to the fact that given a training dataset  $\mathbb{D}_l$  a number of  $\max_{d \in \mathbb{D}_l} \{|V_d|\}$  tables are occupied at most.

## IV. IBGN LEARNING

In what follows we focus on how to learn the network structure and the parameter vectors  $\theta$  and  $\phi$  from the training data  $\mathbb{D}_l$  for a particular complex activity  $l$ .

### A. Learning Network Structure

Instead of configuring a network with chain-based or fully-connected links, we would like to learn a network structure  $\mathbf{G}$  in IBGN according to a score function that best matches the training data  $\mathbb{D}_l$ , i.e., learning from empirical data on which links to select in our constructed networks.

An IBGN model is built over a collection of variables  $\mathbf{t}$  for table assignments,  $\mathbf{a}$  for atomic-action assignments and  $\mathbf{r}$  for relation assignments. In detail, for a specific instance  $d = \langle I_1, I_2, \dots, I_k \rangle$  with  $k = |V_d|$ , its corresponding network involves variables  $\mathbf{t} = \{\mathbf{t}_1, \mathbf{t}_2, \dots, \mathbf{t}_k\}$ ,  $\mathbf{a} = \{\mathbf{a}_1, \mathbf{a}_2, \dots, \mathbf{a}_k\}$ ,  $\mathbf{r} = \{\mathbf{r}_{1,2}, \mathbf{r}_{1,3}, \dots, \mathbf{r}_{1,k}, \mathbf{r}_{2,3}, \mathbf{r}_{2,4}, \dots, \mathbf{r}_{2,k}, \dots, \mathbf{r}_{k-1,k}\}$ ,  $\mathbf{c} = \{\mathbf{c}_{1,2}, \mathbf{c}_{1,3}, \dots, \mathbf{c}_{1,k}, \mathbf{c}_{2,3}, \mathbf{c}_{2,4}, \dots, \mathbf{c}_{2,k}, \dots, \mathbf{c}_{k-1,k}\}$ . To consider a general network structure, we first introduce a *null* interval to make every instance in  $\mathbb{D}_l$  having the same number of  $k^* = \max_{d \in \mathbb{D}_l} \{|V_d|\}$  intervals. A *null* interval is defined as  $(+\infty, \text{null}, +\infty)$  such that its associated atomic action is *null* and its temporal relation with any other intervals is *null*. In other words, *null* can be viewed as a special atomic action class. For any instance of size  $k < k^*$ ,  $k^* - k$  *null* intervals are appended at the rear of the instance. In this way, every instance has the same number of  $k^*$  intervals. Correspondingly,

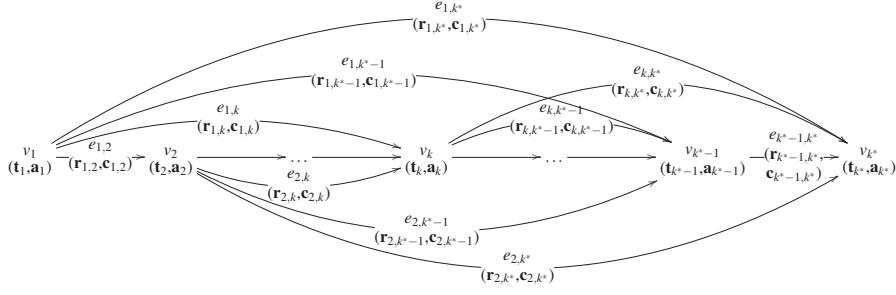


Figure 8. The illustration of the IBGN network structure  $\mathbf{G}$  associated with variables.

any IBGN has a total number of  $(k^* + 1)k^*$  possible random variables, with  $k^*$  possible variables for tables  $\mathbf{t}$ ,  $k^*$  possible variables for atomic actions  $\mathbf{a}$ ,  $\frac{k^*(k^*-1)}{2}$  possible variables for interval relations  $\mathbf{r}$  and  $\frac{k^*(k^*-1)}{2}$  possible variables for interval relation constraints  $\mathbf{c}$ . An exemplar IBGN model can be described in Figure 8, where each  $v_i$  is associated with variables  $\mathbf{t}_i$  and  $\mathbf{a}_i$ , and each  $e_{i,j}$  is associated with variable  $\mathbf{r}_{i,j}$  and  $\mathbf{c}_{i,j}$ , with  $1 \leq i \leq j \leq k^*$ . To this end, our IBGN structure learning problem is defined as to find a  $\mathbf{G} = (V_{\mathbf{G}}, E_{\mathbf{G}})$  such that the score of  $\mathbf{G}$  given  $\mathbb{D}_l$  is maximum.

Next, we employ *structure constraints* to translate the IBGN model to a corresponding problem in Bayesian networks.

**Definition 2.** Given an IBGN model  $\mathbf{G}$ , its corresponding Bayesian network is defined as a directed bipartite graph  $\mathbf{G}' = (V_{\mathbf{G}'}, E_{\mathbf{G}'})$  where  $V_{\mathbf{G}'} = U_{\mathbf{G}'} \cup W_{\mathbf{G}'}$ , with the structure constraints such that

- (1)  $|U_{\mathbf{G}'}| = k^*$ ,  $|W_{\mathbf{G}'}| = k^*(k^* - 1)/2$ ,
- (2)  $\forall v' \in U_{\mathbf{G}'} : \widehat{v}' = M + 1$ ,  $\forall v' \in W_{\mathbf{G}'} : \widehat{v}' = 8$ ,
- (3)  $\forall v' \in U_{\mathbf{G}'} : \text{in-degree}(v') = 0$ ,  $\forall v' \in W_{\mathbf{G}'} : \text{in-degree}(v') = 0$  or  $2$ ,

where  $\widehat{v}'$  denotes the number of distinct elements of  $v'$ .

A node  $v'_n$  in  $U_{\mathbf{G}'}$  ( $1 \leq n \leq |U_{\mathbf{G}'}|$ ) maps to the variable  $\mathbf{a}_n$  in  $\mathbf{G}$ , while a node  $v'_{n',n}$  in  $W_{\mathbf{G}'}$  ( $1 \leq n' < n \leq |U_{\mathbf{G}'}|$ ) maps to the variable  $\mathbf{r}_{n',n}$  in  $\mathbf{G}$ . That is,  $U_{\mathbf{G}'} = \{\mathbf{a}_1, \dots, \mathbf{a}_{k^*}\}$  and  $W_{\mathbf{G}'} = \{\mathbf{r}_{1,2}, \mathbf{r}_{1,3}, \dots, \mathbf{r}_{1,k^*}, \dots, \mathbf{r}_{k^*-1,k^*}\}$ . Notice that a *null* is introduced to represent the absence of a node or a relation in an instance of  $\mathbb{D}_l$  (constraint (2)), and thus there are  $M + 1$  possible atomic-action assignments for a node in  $U_{\mathbf{G}'}$  and  $|\mathbb{R}| + 1 = 8$  possible relation assignments for a node in  $W_{\mathbf{G}'}$ . Moreover, any node  $v'_n$  in  $U_{\mathbf{G}'}$  has no parent, and any node  $v'_{n',n}$  in  $W_{\mathbf{G}'}$  has either being connected to the nodes  $v'_{n'}$  and  $v'_n$  in  $U_{\mathbf{G}'}$  or not being connected to any node (constraint (3)). That means a link  $e_{n',n}$  exists in  $\mathbf{G}$  if and only if its corresponding node  $v'_{n',n}$  in  $\mathbf{G}'$  has  $\text{in-degree}(v'_{n',n}) = 2$ . The structure of  $\mathbf{G}'$  associated with the variables is illustrated in Figure 9.

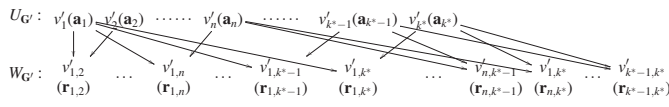


Figure 9. The corresponding bipartite graph  $\mathbf{G}'$  of the IBGN structure  $\mathbf{G}$ .

Now, the problem of determining whether a link should exist in IBGN is converted to the problem of finding a set of

links  $E_{\mathbf{G}'}$  with the maximal score under the above constraints. In particular, we consider the Bayesian Information Criterion (BIC) as the score function, which addresses the overfitting issue by introducing a penalty term in the structure, as proved in the Appendix B:

$$\begin{aligned} \text{BIC-Score}(\mathbf{G} : \mathbb{D}_l) &= \text{BIC-Score}(\mathbf{G}' : \mathbb{D}_l) + \lambda \\ &= \max_{\Phi} \log \prod_{i=1}^{|W_{\mathbf{G}'}} \prod_{j=1}^{|\widehat{\Pi}_i|} \prod_{k=1}^8 \phi_{ijk}^{n'_{ijk}} - \frac{\log |\mathbb{D}_l|}{2} \cdot \sum_{i=1}^{|W_{\mathbf{G}'}} 7 \cdot \widehat{\Pi}_i + \lambda, \end{aligned} \quad (3)$$

where  $\lambda$  is a constant.  $\Pi_i$  denotes the parents of the  $i$ -th node in  $W_{\mathbf{G}'}$  and  $\widehat{\Pi}_i = (M + 1)^{|\Pi_i|}$ , which is the number of possible instantiations of the parent set  $\Pi_i$  of the  $i$ -th node. In fact,  $\widehat{\Pi}_i = 1$  or  $(M + 1)^2$ . For example, suppose  $v'_{n',n}$  be the  $i$ -th node in  $W_{\mathbf{G}'}$  and  $v'_{n'}, v'_n \in U_{\mathbf{G}'}$ . If the links  $v'_{n'} \rightarrow v'_{n',n}$  and  $v'_n \rightarrow v'_{n',n}$  exist in  $E_{\mathbf{G}'}$  (i.e.  $\text{in-degree}(v'_{n',n}) = 2$ ), then the node  $v'_{n',n}$  has two parents (i.e.  $\Pi_i = \{v'_{n'}, v'_n\}$ ) whose number of categories is  $(M + 1)$ , and thus  $\widehat{\Pi}_i = (M + 1)^2$ ; otherwise,  $\widehat{\Pi}_i = 1$ . In addition,  $\Phi$  is the parameter vector such that  $\forall_{ijk} : \phi_{ijk} = P(x_{ik} | \pi_{ij})$ , where  $x_{ik}$  and  $\pi_{ij}$  denotes that the  $i$ -th node in  $W_{\mathbf{G}'}$  is assigned with the  $k$ -th element and its parent nodes are assigned with the  $j$ -th element (i.e. an instantiation of its parent set  $\Pi_i$ ), respectively;  $n'_{ijk}$  indicates how many instances of  $\mathbb{D}_l$  contain both  $x_{ik}$  and  $\pi_{ij}$ . Note that any node  $v'_{n',n} \in W_{\mathbf{G}'}$  has eight elements (i.e.  $\widehat{v'_{n',n}} = 8$ ). At this stage, several techniques can be employed to learn the structure of  $\mathbf{G}'$  efficiently [5], [10], [16]. After finding the best structure  $\mathbf{G}^{I*} = \arg \max \text{BIC-Score}(\mathbf{G}' : \mathbb{D}_l)$ , a link  $e_{n',n}$  is in  $\mathbf{G}$  if and only if  $\text{in-degree}(v'_{n',n} \in W_{\mathbf{G}^{I*}}) = 2$ .

### B. Learning Parameters

We first estimate the parameters  $\theta = \{\theta_1, \theta_2, \dots, \theta_\ell\}$  for node generation. Since the variable  $\mathbf{t}_n$  is latent for each node  $v_n$  in our generative process, we shall approximately estimate the posterior distribution on  $\mathbf{t}$  by Gibbs sampling. Formally, we marginalize the joint probability in Eq.(2) and derive the posterior probability of latent variable  $\mathbf{t}_n$  being assigned to the table  $T_\zeta$  ( $1 \leq \zeta \leq \ell$ ) as follows:

$$P(\mathbf{t}_n = T_\zeta | \mathbf{t}_{-n}, \mathbf{a}, \mathbf{r}; \alpha, \beta) \propto \frac{na_{\zeta, \bar{i}-n} + \beta_{\zeta, \bar{i}}}{\sum_{i'=1}^M (na_{\zeta, i', -n} + \beta_{\zeta, i'})} \times \begin{cases} \frac{m_{\zeta}}{n + \alpha_{\zeta} - 1} & \text{if } \zeta \leq NT_n \\ \frac{\alpha_{\zeta}}{n + \alpha_{\zeta} - 1} & \text{if } \zeta = NT_n + 1 \end{cases}$$

where  $na_{\zeta, i'}$  is the count that nodes have been assigned to the atomic action type  $A_{i'}$  at the table  $T_\zeta$ , and  $nt_\zeta$  is the count of nodes in  $G_d$  that has been assigned to the table  $T_\zeta$ .  $\bar{i}$  refer to

the atomic action assignments for nodes  $v_n$ .  $NT_n$  is the count of occupied tables with  $\sum_{i=1}^{NT_n} nt_i = n - 1$ . The suffix  $-n$  of  $na$  means the count that does not include the current assignment of table for the node  $v_n$ .  $\alpha_\zeta$  is the tuning parameter for the  $\zeta$ -th table selection during *CRP*;  $\beta_{\zeta,i}$  is the Dirichlet prior for the  $i$ -th atomic action conditioned on the  $\zeta$ -th table. We provide the detailed derivations of the Gibbs sampling in Appendix C. By sampling the latent tables following the above distribution, the distributions of  $\theta_\zeta$  ( $1 \leq \zeta \leq \ell$ ) can be estimated as

$$\theta_{\zeta,i}^* = \frac{na_{\zeta,i} + \beta_{\zeta,i}}{\sum_{i'=1}^M (na_{\zeta,i'} + \beta_{\zeta,i'})}, \text{ for each } 1 \leq i \leq M.$$

Normally, the hyperparameters  $\alpha$  and  $\beta$  are set as fixed values before the execution of a Gibbs sampler. In our IBGN model,  $\alpha$  and  $\beta$  involve a number of  $\ell$  and  $\ell M$  prior parameters, respectively. As they are unfortunately unknown beforehand, it is difficult to manually encode each parameter to proper values. As a result, we need to instead learn each hyperparameter to obtain reasonable results. The adoption of Gibbs sampling enables us to seamlessly incorporate the tuning of these hyperparameters as presented in Algorithm 2. The stop condition may be that a predefined max iterations

---

**Algorithm 2** Gibbs Sampling Algorithm with Hyperparameter Tuning Method Embedded.

---

```

1: procedure GIBBS_SAMPLER_WITH_HYPERPARAMETER_ESTIMATE
2:    $s = 0$ ; ▷ The initial iteration of the Gibbs sampler.
3:   Initialize the values of  $\alpha$  and  $\beta$ ;
4:   repeat
5:      $s \leftarrow s + 1$ ; ▷ The  $s$ -th iteration of the Gibbs sampler.
6:     Get the samples of latent tables generated by the Gibbs sampler at current
       iteration;
7:     Update hyperparameters  $\alpha^{new} = f(\alpha)$ ,  $\beta^{new} = g(\beta)$ ;
8:   until termination conditions are reached;
9: end procedure

```

---

has been reached or that an estimation function converges to a given threshold. To update the hyperparameters  $\alpha$  and  $\beta$ , a convergent method proposed by Minka [19] is used as follows:

$$\alpha_\zeta^{(s+1)} = f(\alpha_\zeta) = \alpha_\zeta \times \frac{\sum_s \Psi(\sum_{d \in \mathbb{D}_l} nt_\zeta^{(s)} + \alpha_\zeta) - \Psi(\alpha_\zeta)}{\sum_s \Psi(\sum_{d \in \mathbb{D}_l} |V_d| + \sum_{\zeta'=1}^\ell \alpha_{\zeta'}) - \Psi(\sum_{\zeta'=1}^\ell \alpha_{\zeta'})},$$

$$\beta_{\zeta,i}^{(s+1)} = g(\beta_{\zeta,i}) = \beta_{\zeta,i} \times \frac{\sum_s \Psi(na_{\zeta,i}^{(s)} + \beta_{\zeta,i}) - \Psi(\beta_{\zeta,i})}{\sum_s \Psi(\sum_{i'=1}^M (na_{\zeta,i'}^{(s)} + \beta_{\zeta,i'})) - \Psi(\sum_{i'=1}^M \beta_{\zeta,i'})},$$

where  $\Psi$  is digamma function, and the superscript  $(s)$  indicates the sample generated by the Gibbs sampler at the  $s$ -th iteration.

Next, we estimate the parameters  $\phi = \{\phi_{i,j,z} : 1 \leq i, j \leq M, 1 \leq z \leq |C|\}$  for link generation. It can be seen that the probability distribution of variable  $\mathbf{r}_{n',n}$  relies on the triplet  $(A_i, A_j, C_z)$  only (where  $\mathbf{a}_{n'} = A_i$ ,  $\mathbf{a}_n = A_j$  and  $\mathbf{c}_{n',n} = C_z$ ), and thus we can learn these parameters by maximum likelihood estimate method. In our IBGN model, given a triplet  $(A_i, A_j, C_z) \in \mathbb{A} \times \mathbb{A} \times \mathbb{C}$ , the conditional probability distribution on  $\mathbf{r}_{n',n}$  is a multinomial over all possible relations in  $C_z$ . Then, the likelihood of the parameter  $\phi_{i,j,z}$  for  $P(\mathbf{r}_{n',n} | A_i, A_j, C_z)$  with respect to  $\mathbb{D}_l$  is:

$$L(\phi_{i,j,z}; \mathbb{D}_l) = \prod_{d \in \mathbb{D}_l} P(\mathbf{r}_{n',n} | A_i, A_j, C_z; \phi_{i,j,z}) = \prod_{r=1}^{|C_z|} \phi_{i,j,z,r}^{nr_{i,j,z,r}}, \quad (4)$$

By applying a Lagrange multiplier to ensure  $\sum_{r=1}^{|C_z|} \phi_{i,j,z,r} = 1$ , maximum likelihood estimate for  $\phi_{i,j,z,r}$  is

$$\phi_{i,j,z,r}^* = \frac{nr_{i,j,z,r}}{\sum_{r'=1}^{|C_z|} nr_{i,j,z,r'}}, \quad (5)$$

where  $nr_{i,j,z,r}$  is the number of links  $e_{n',n}$  are labeled with the  $r$ -th relation in  $\mathbb{D}_l$ , with  $\mathbf{a}_{n'} = A_i$ ,  $\mathbf{a}_n = A_j$ ,  $\mathbf{c}_{n',n} = C_z$  and  $e_{n',n} \models \mathbf{G}^*$ . Note the trivial cases of  $\phi_{i,j,z,r}^* = 1$  for  $1 \leq z \leq 7$  as each of them contains only one element as indicated in Figure 6.

Now, by integrating out the latent variable  $\mathbf{t}$  with all the parameters derived above, the probability of the occurrence of a new instance given the  $l$ -th type of complex activity is estimated below

$$P(\mathbf{a}', \mathbf{r}'; \mathbb{D}_l) = \prod_i \left( \sum_{\zeta} \theta_{\zeta,i} \right) \times \prod_{i,j,z,r \models \mathbf{G}^*} \phi_{i,j,z,r}, \quad (6)$$

where  $\mathbf{a}'$  and  $\mathbf{r}'$  are the sets of atomic actions and their relations in the new instance, respectively, and  $i, j, z, r \models \mathbf{G}^*$  indicate only these links obeying the structure of  $\mathbf{G}^*$  are counted. To predict which type of complex activity a new instance belongs to, we simply evaluate the posterior probabilities over each of the  $L$  possible types of complex activities as

$$l^* = \arg \max_{1 \leq l \leq L} P(\mathbf{a}', \mathbf{r}'; \mathbb{D}_l). \quad (7)$$

## V. EXPERIMENTS

Experiments are carried out on three benchmark datasets as well as our in-house dataset on recognizing complex hand activities. In addition to the proposed approach **IBGN**, two variants with fixed network structures are also considered: One is **IBGN-C** for chain-based structures, where only the links between two neighbouring nodes in networks are constructed; The other one is **IBGN-F** for fully-connected structures, where all pairwise links in networks are constructed. Several well-established models are employed as the comparison methods, which include IHMM [20], dynamic Bayesian network (DBN) [12] and ITBN [31], where IHMM and DBN are implemented on our own, and ITBN is obtained from the authors. All internal parameters are tuned for best performance for a fair comparison. The standard evaluation metric of *accuracy* is used, which is computed as the proportion of correct predictions.

a) *Experimental Set-Ups*: The Raftery and Lewis diagnostic tool [24] is employed to detect the convergence of the Gibbs sampler (Algorithm 2) for the IBGN family. It has been observed that overall we have a short burn-in period, which suggests the Markov chain samples are mixing well. Thus  $nt$  and  $na$  are set to the averaged counts of their first 1000 samples after convergence. In addition, we utilize the branch-and-bound algorithm [5] for constraints-based structure learning. This approach can strongly reduce the time and memory costs for learning Bayesian network structures based on the BIC score function (Eq. (3)) without losing global optimality guarantees. Besides, to avoid the division-by-zero issue in practice (i.e.  $\sum_{r'=1}^{|C_z|} nr_{i,j,z,r'} = 0$  in Eq. (5)), we instead use  $\phi_{i,j,z,r}^* = \frac{nr_{i,j,z,r} + \rho}{\sum_{r'=1}^{|C_z|} nr_{i,j,z,r'} + \rho |C_z|}$  by introducing a small smoothing constant  $\rho$  ( $\rho = 10^{-5}$ ) in the following experiments.

b) *Time Complexity Analysis*: The time complexities of IBGN-C and IBGN-F are  $O(M^2 + |\mathbb{D}_l|T_n\ell^2)$  for training each complex activity category, where  $T_n$  is the number of iterations executed in Algorithm 2. IBGN has an extra time complexity of  $O(\sum_{p=0}^{\log_2 K} \binom{K}{p})$  for structure learning, where  $K = \frac{k^*(k^*-1)}{2}$ . On the other hand, the time complexities of the IBGN family at the testing stage are the same, which is  $O(M\ell)$  for a single test instance.

#### A. Experiments on Three Existing Benchmark Datasets

a) *Datasets and Preprocessing*: The three publicly-available complex activity recognition datasets collected from different types of cameras and sensors are considered, as summarized in Table. II. We employ these datasets in our evaluation due to their distinctive properties: The OSUPEL dataset [3] can be used to evaluate the case where only a handful of atomic action types and simple relations are recorded; Opportunity [25] is challenging as it contains a large number of atomic action types and also involves intricate interval relations in instances; CAD14 [15] represents the datasets having relatively larger number of complex activity categories.

Table II  
SUMMARY OF THE PUBLICLY AVAILABLE DATASETS.

	OSUPEL	Opportunity	CAD14
Application type	Basketball play	Daily living	Composable activities
Recording devices	one ordinary camera	72 on-body sensors of 10 modalities	one RGB-D camera
E.g. of atomic actions	shoot, jump, dribble, etc.	sit, open door, wash cup, etc.	clap, talk phone, walk, etc.
E.g. of complex activities	two offensive play types	relax, cleanup, coffee time, early morning, sandwich time	talk and drink, walk while clapping, talk and pick up, etc.
No. of atomic action types	6	211	26
No. of complex activity types	2	5	16
No. of instances	72	125	693
No. of intervals per instance	2-5	1-78	3-11

To recognize atomic actions in each dataset, we adopt the methods developed in their respective corresponding work. That is, we employed the dynamic Bayesian network models that are used to model and recognize each atomic action including shoot, jump, dribble and so on for OSUPEL [31]. Similarly, for CAD14 [15] we adopted the hierarchical discriminative model to recognize atomic action such as clap, talk phone and so on through an discriminative pose dictionary. For the sensor-based Opportunity dataset, we utilized the activity recognition chain system (ARC) [4] to recognize atomic action recognition from sensors. It is worth mentioning that we can also recognize *null* type of complex activity by labeling the intervals that are not annotated to any activities in the datasets.

b) *Comparison under an Ideal Condition*: First of all, the competing models are evaluated under the condition that all intervals are correctly detected. Table III displays the averaged accuracy results over 5-fold cross-validations, where the proposed IBGN family clearly outperforms other methods with a big margin on all three datasets. The reason is that IBGNs engage the rich interval relations among atomic actions. Although ITBN can also encode relations, it however

fails with the multiple occurrences of the same atomic actions or when inconsistent relations existing among training instances. As a considerable amount of multiple occurrences of the same atomic actions and inconsistent temporal relations exist in CAD14, ITBN performs the worst. It can also be seen that IBGN-F with fully-connected relations performs better than IBGN-C on the Opportunity and CAD14 datasets where relations are intricate. However, IBGN-F might be overfitted when relations are simple, e.g. the OSUPEL dataset. Overall IBGN outperforms its two variants by its ability to adaptively learn network structures from data, where fixed structures might face the issue of either overfitting or underfitting.

Table III  
ACCURACY COMPARISON ON DIFFERENT DATASETS.

	IHMM	DBN	ITBN	IBGN-C	IBGN-F	IBGN
OSUPEL	0.53	0.58	0.69	0.79	0.76	<b>0.81</b>
Opportunity	0.74	0.83	0.88	<b>0.98</b>	0.96	<b>0.98</b>
CAD14	0.93	0.95	0.51	0.97	<b>0.98</b>	<b>0.98</b>

c) *Robustness Tests under Atomic-Level Errors*: In practice the accuracy of atomic action recognition will significantly affect complex activity recognition results. To evaluate the performance robustness, we also compare the competing models under atomic action recognition errors. First, it is important to check whether our model is robust under label perturbations of atomic-action-level (or atomic-level for short). To show this, we synthetically perturb the atomic-level predictions. Figure 10 reports the comparison results on Opportunity under two common atomic-level errors. It can be seen that IBGNs are more robust to misdetection errors where atomic actions are not detected or are falsely recognized as another actions. We perturbed the true labels with error rates ranging from 10-30 percents to simulate synthetic misdetection errors. Similarly, we also perturbed the start and end time of intervals with noises of 10-30 percents to simulate duration-detection errors where interval durations are falsely detected. It is also clear that IBGNs outperform other competing models under duration-detection errors.

In addition, we report the evaluated performances under real detected errors caused by the ARC system for atomic-level recognition. We chose three classifiers for atomic action recognition from the ARC system, i.e. kNN, SVM and DT. Features such as mean, variance, correlation and so on are selected by setting a time-sliced window of 1s. After classification, each interval is assigned to an atomic action type. As shown in Figure 10, the models which can manage interval relations are relatively more robust to the atomic-level errors than other models, such as ITBN and IBGNs. Moreover, it is evident that IBGNs are noticeably more robust than ITBN with around 15% – 87% performance boost. IBGN performs the best among its family because it is more capable of handling the structural variability in complex activities than the other two variants, which may avoid more noise existing in training and testing information. Note similar conclusions are also obtained on the OSUPEL and CAD14 datasets.



atomic-level error rate	recognition accuracy					
	IHMM	DBN	ITBN	IBGN-C	IBGN-F	IBGN
under synthetic atomic-level misdetection errors						
0.1	0.31	0.73	0.79	0.92	0.88	<b>0.94</b>
0.2	0.29	0.67	0.74	<b>0.87</b>	<b>0.87</b>	<b>0.87</b>
0.3	0.22	0.65	0.71	0.83	<b>0.84</b>	<b>0.84</b>
under synthetic atomic-level duration detection errors						
0.1	0.16	0.45	0.76	0.83	0.88	<b>0.89</b>
0.2	0.16	0.45	0.72	0.83	<b>0.85</b>	<b>0.85</b>
0.3	0.16	0.45	0.69	0.82	<b>0.83</b>	<b>0.83</b>
under real atomic-level detected errors						
0.165 (kNN)	0.66	0.62	0.54	<b>0.91</b>	0.79	<b>0.91</b>
0.242 (SVM)	0.58	0.54	0.46	0.83	0.71	<b>0.85</b>
0.315 (DT)	0.16	0.04	0.38	<b>0.71</b>	0.54	<b>0.71</b>

Figure 10. Accuracies under atomic-level errors on Opportunity dataset.

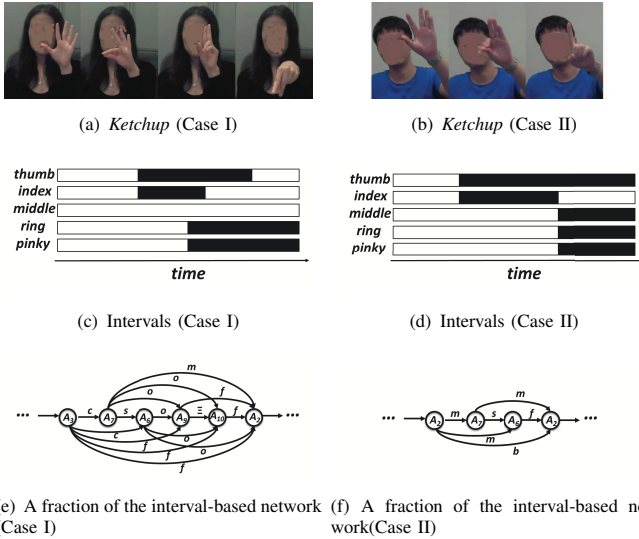


Figure 11. Two instances of the complex activity ASL word *ketchup*.  $A_1$ - $A_5$  refer to the straightening state of thumb, index, middle, ring and pinky fingers, respectively (white bars), while  $A_6$ - $A_{10}$  refer to the bending state of these fingers (black bars).

## B. Our Complex Hand Activity Dataset

a) *Data Collection*: We propose a new complex activity dataset on depth camera-based complex hand activities on performing American Sign Language (ASL). It is an ongoing effort, and at the moment it contains 3,480 annotated instances, which is already about 5-fold larger than existing ones. As illustrated in Fig. 11, complex activities in our dataset are defined as selected ASL hand-actions. There are 20 atomic actions, which are defined as the states of individual fingers, either straight or bent. It is important to realize that in a complex activity, there could be multiple occurrences of the same atomic action, as is also exemplified in Fig. 11(f) where an action  $A_2$  appears twice in the sub-network.

Sixteen subjects participate in the data collection, with various factors being taken into consideration to add to the data diversities. Subjects of different genders, ages groups, races are present in the dataset. The male to female ratio is 12 to 4, races ratio is 14 to 2 and participants' ages span from around 15 to 40. For each subject, the depth image sequences are recorded with a front-mount SoftKinetic camera while performing designated complex activities in office settings,

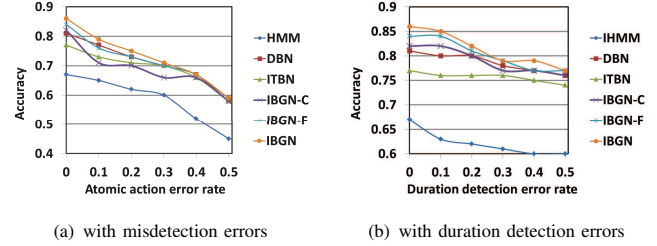


Figure 12. Performance changes vs. perturbation of atomic-action-level errors.

with a frame-rate of 25 FPS, image size of  $320 \times 240$ , and hand-camera distance of around 0.6-1m. In total, the dataset contains 19 ASL hand-action complex activities, with each having 145-290 instances collected among all subjects. Each of the instance is comprised of 5-17 atomic action intervals. The 19 ASL hand-actions are *air*, *alphabets*, *bank*, *bus*, *gallon*, *high school*, *how much*, *ketchup*, *lab*, *leg*, *lady*, *quiz*, *refrigerator*, *several*, *sink*, *stepmother*, *teaspoon*, *throw*, *xray*.

b) *Atomic Hand Action Detection*: To detect atomic-level hand-actions, we make use of the existing hand pose estimation system [30] with a postprocessing step to map joint location prediction outputs to the bent/straight states of fingers. To evaluate performance of the interval-level atomic action detection results, we follow the common practice and use the intersection-over-union of intervals with a 50% threshold to identify a hit/false alarm/missing, respectively. Finally F1 score is used based on the obtained precision and recall values. Note here the finger bent states are considered as foreground intervals.

c) *Robustness Tests under Atomic-Level Errors*: We first evaluate the performance on simulated synthetic misdetection errors and duration-detection errors. From Fig. 12, we observe that overall IBGN is notably more robust than other approaches, meanwhile IHMM consistently produces the worst results. Our model is relatively robust in the presence of atomic-level errors.

Now we are ready to show the performance of our model when working with our atomic-level predictor as mentioned previously. Overall our atomic-level predictor achieves F1 score of 0.724. Table IV summarizes the final accuracy comparisons of the six competing approaches based on our atomic-level predictor vs. the atomic-level ground-truth labels on our hand-action dataset. It is not surprising that in both scenarios IBGN again significantly outperforms the rest approaches. It is worth noting that taking into account the challenging task of atomic-level hand pose estimation on its own, the gap in performances of 0.58 vs. 0.86 on predicting over 19 complex activity categories is reasonably, which is also certainly one thing we should improve over in the future. Fig. 13 presents the confusion matrix of IBGN working with our atomic-level predictor. We observe that our system is able to recognize the ASL words such as *xray*, *alphabets* and *quiz* very well. At the same time, several ASL words turn to be difficult to deal with, with accuracy under 50%. This may mainly due to the relatively low accuracy of the atomic-level predictor we are using on the particular atomic actions.

Table IV  
COMPLEX ACTIVITY ACCURACY COMPARISONS ON OUR HAND-ACTION DATASET.

IHMM	DBN	ITBN	IBGN-C	IBGN-F	IBGN
with real atomic-level prediction					
0.43	0.51	0.54	0.49	0.55	<b>0.58</b>
with atomic-level ground-truth (ideal situation)					
0.67	0.81	0.77	0.82	0.84	<b>0.86</b>

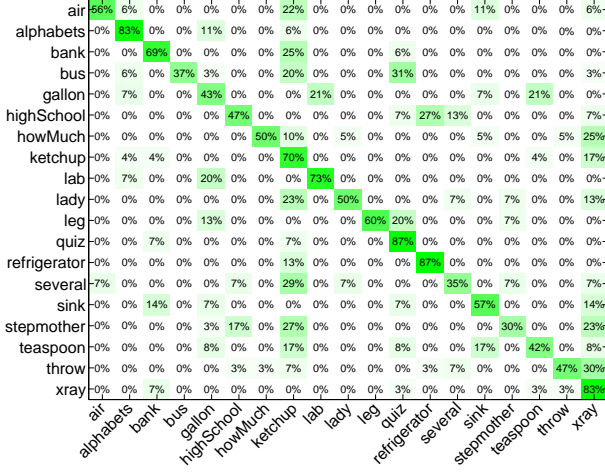


Figure 13. Confusion matrix of IBGN on our hand-action dataset.

## VI. CONCLUSION

We present an interval-based Bayesian generative network approach to account for the latent structures of complex activities by constructing probabilistic interval-based networks with temporal dependencies in complex activity recognition. In particular, the Bayesian framework and the novel application of Chinese restaurant process (CRP) of our IBGN model enable us to explicitly capture inherit structural variability in each of the complex activities. In addition, we make publicly available a new complex hand activity dataset dedicated to the purpose of complex activity recognition, which contains around an-order-of-magnitude larger number of annotated instances. Experimental results suggest our proposed model outperforms existing state-of-the-arts by a large margin in a range of well-known testbeds as well as our new dataset. It is also shown that our approach is rather robust to the errors introduced by the low-level atomic action predictions from raw signals. As part of future work, we are considering relaxing the assumption that the IBGN models share the same structure for representing multiple instances of the same complex activity, and will instead learn more flexible structures for each class of complex activities by introducing latent structure variables that decide whether a link should exist in an instance. Also, we will continue the finalization of our hand-action dataset, improving the atomic-level atomic action prediction method, as well as attempting toward the establishment of standardized comparisons on existing systems.

## VII. ACKNOWLEDGMENTS

This research was supported in part by grant CQU903005203326 from the Fundamental Research Funds for the Central Universities in China, grants R-252-000-473-133 and R-252-000-473-750 from the National University of Singapore, and A\*STAR JCO grants 15302FG149 and 1431AFG120.

## APPENDIX A PROOFS OF THEOREM 1

We first prove that the composition operation  $\circ$  on the interval relation union set  $\mathbb{S}$  satisfies the associative law. The set of all the 127 unions is denoted by  $\mathbb{S}$ .

**Definition 3. (Composition Product of Two Relation Sets)** The composition product of two sets of interval relations  $R, R' \in \mathbb{S}$ , i.e.  $R = \{r_1, \dots, r_{|R|}\}$  and  $R' = \{r'_1, \dots, r'_{|R'|}\}$ , where any  $r_i, r'_j \in \mathbb{R}$ , is defined as  $R \circ R' = \bigcup_{i,j} (r_i \circ r'_j)$ .

**Lemma 2. (Associative Law on Composition)**

$$(\mathbf{R}_x \circ \mathbf{R}_y) \circ \mathbf{R}_z = \mathbf{R}_x \circ (\mathbf{R}_y \circ \mathbf{R}_z), \quad \text{for any } \mathbf{R}_x, \mathbf{R}_y, \mathbf{R}_z \in \mathbb{S}.$$

*Proof.* Let  $\mathbf{R}_x = \{r_{x,1}, \dots, r_{x,X}\}$ ,  $\mathbf{R}_y = \{r_{y,1}, \dots, r_{y,Y}\}$  and  $\mathbf{R}_z = \{r_{z,1}, \dots, r_{z,Z}\}$ , where any  $r_{i,j} \in \mathbb{R}$ . Then,  $(\mathbf{R}_x \circ \mathbf{R}_y) \circ \mathbf{R}_z = (\bigcup_{i,j} (r_{x,i} \circ r_{y,j})) \circ \mathbf{R}_z = \bigcup_k ((\bigcup_{i,j} (r_{x,i} \circ r_{y,j})) \circ r_{z,k}) = \bigcup_{i,j,k} ((r_{x,i} \circ r_{y,j}) \circ r_{z,k})$  and  $\mathbf{R}_x \circ (\mathbf{R}_y \circ \mathbf{R}_z) = \mathbf{R}_x \circ (\bigcup_{j,k} (r_{y,j} \circ r_{z,k})) = \bigcup_i (r_{x,i} \circ (\bigcup_{j,k} (r_{y,j} \circ r_{z,k}))) = \bigcup_{i,j,k} (r_{x,i} \circ (r_{y,j} \circ r_{z,k}))$ . Since the composition on the seven interval relation set satisfies the associative law that is both left and right associative, the associative law also holds on  $\mathbb{R}$ , which is closed under the composition operation, i.e.  $(r_x \circ r_y) \circ r_z = r_x \circ (r_y \circ r_z)$ , for any  $r_x, r_y, r_z \in \mathbb{R}$ . So, we have  $(\mathbf{R}_x \circ \mathbf{R}_y) \circ \mathbf{R}_z = \mathbf{R}_x \circ (\mathbf{R}_y \circ \mathbf{R}_z)$ .  $\square$

**Lemma 3. (Path Consistency)**

Given an IBGN  $G_d$ , if  $\mathbf{x}_{i,k} \in \mathbf{x}_{i,j} \circ \mathbf{x}_{j,k}$  for any  $1 \leq i < j < k \leq |V_d|$ , then for any path  $\mathbf{P} = v_i \rightarrow v_{j'} \rightarrow v_{j''} \rightarrow \dots \rightarrow v_{k'} \rightarrow v_k$  in  $G_d$ ,  $\mathbf{x}_{i,k} \in \mathbf{x}_{i,j'} \circ \mathbf{x}_{j',j''} \circ \dots \circ \mathbf{x}_{k',k}$ .

*Proof.* For any path  $\mathbf{P} = v_i \rightarrow v_{j'} \rightarrow v_{j''} \rightarrow \dots \rightarrow v_{k'} \rightarrow v_k$  in  $G_d$ , we have  $\mathbf{x}_{i,k} \in \mathbf{x}_{i,j'} \circ \mathbf{x}_{j',k}$  and  $\mathbf{x}_{j',k} \in \mathbf{x}_{j',j''} \circ \mathbf{x}_{j'',k}$ , then  $\mathbf{x}_{i,k} \in \mathbf{x}_{i,j'} \circ (\mathbf{x}_{j',j''} \circ \mathbf{x}_{j'',k}) \in \mathbf{x}_{i,j'} \circ \mathbf{x}_{j',j''} \circ \mathbf{x}_{j'',k}$ . Iteratively, we finally have  $\mathbf{x}_{i,k} \in \mathbf{x}_{i,j'} \circ \mathbf{x}_{j',j''} \circ \dots \circ \mathbf{x}_{k',k}$ .  $\square$

*Proof.*

**(Consistency)**

Lemma 3 indicates that if any  $\Delta ijk$  in the network satisfies the transitivity properties, then any path in the network also satisfies the transitivity properties. Hence, the entire network generated through our construction is consistent.

**(Completeness)**

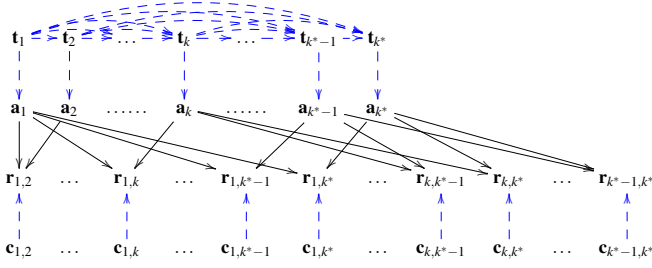
(by contradiction)

Suppose there exists one interval relations  $\mathbf{x}_{i,n}$  that cannot be generated through our construction, i.e.  $\mathbf{x}_{i,n} \notin \bigcap_{j=i+1}^{n-1} (\mathbf{x}_{i,j} \circ \mathbf{x}_{j,n})$ , which means there exists at least one  $j^*$  ( $1 \leq j^* \leq n-1$ ) that  $\mathbf{x}_{i,n} \notin \mathbf{x}_{i,j^*} \circ \mathbf{x}_{j^*,n}$ . This contradicts the fact that the network is consistent. Besides, any possible relation in  $\mathbb{R}$  can be generated between two neighboring nodes. That is to say, any possible triangle that is consistent can be generated by our model.  $\square$

## APPENDIX B

PROOF OF  $\text{BIC-Score}(\mathbf{G} : \mathbb{D}) = \text{BIC-Score}(\mathbf{G}' : \mathbb{D}) + \lambda$

*Proof.* The corresponding variable dependence in the IBGN model  $\mathbf{G}$  is shown as follows:



According to our definition of the generative process, the structure between  $\mathbf{t}$  and  $\mathbf{a}$  (marked as blue line), the structure among  $\mathbf{t}$  and the structure between  $\mathbf{c}$  and  $\mathbf{r}$  (marked as blue dotted line) are fixed. We only need to learn the structure between  $\mathbf{a}$  and  $\mathbf{r}$ .

In effect, the structure without  $\mathbf{t}$  and  $\mathbf{c}$  and their associated links (blue dotted lines) is equivalent to the Bayesian structure  $\mathbf{G}'$  defined in Definition 2, where  $U_{\mathbf{G}'} = \{\mathbf{a}_1, \mathbf{a}_2, \dots, \mathbf{a}_{k^*}\}$  and  $W_{\mathbf{G}'} = \{\mathbf{r}_{1,2}, \mathbf{r}_{1,3}, \dots, \mathbf{r}_{1,k^*}, \dots, \mathbf{r}_{k^*-1,k^*}\}$  (constraint (1)). The number of categories of any atomic action variable  $\mathbf{a}_i$  ( $1 \leq i \leq k^*$ ) is  $M+1$ , including the *null* atomic action. Similarly, the number of categories of any relation variable  $\mathbf{r}_{i,j}$  ( $1 \leq i < j \leq k^*$ ) is 8, including the *null* relation (constraint (2)). Given a training dataset  $\mathbb{D}$ , for any instance  $d \in \mathbb{D}$  and its corresponding network  $G_d$ , if  $j > |V_d|$ , then  $\mathbf{a}_j = \text{null}$  and  $\mathbf{r}_{i,j} = \text{null}$ . Moreover, any atomic action variable  $\mathbf{a}_i$  has no parent, and any relation variable  $\mathbf{r}_{i,j}$  has either two parents or zero parents (constraint (3)). That is, a link  $e_{i,j}$  exists in  $\mathbf{G}$  if and only if both  $\mathbf{a}_i$  and  $\mathbf{a}_j$  are connected with  $\mathbf{r}_{i,j}$  in  $\mathbf{G}'$ .

Formally, let  $V_{\mathbf{G}} = V_{\mathbf{t}} \cup V_{\mathbf{a}} \cup V_{\mathbf{r}} \cup V_{\mathbf{c}}$  where  $V_{\mathbf{t}} = \{\mathbf{t}_1, \dots, \mathbf{t}_{k^*}\}$ ,  $V_{\mathbf{a}} = \{\mathbf{a}_1, \dots, \mathbf{a}_{k^*}\}$ ,  $V_{\mathbf{r}} = \{\mathbf{r}_{1,2}, \mathbf{r}_{1,3}, \dots, \mathbf{r}_{1,k^*}, \dots, \mathbf{r}_{k^*-1,k^*}\}$  and  $V_{\mathbf{c}} = \{\mathbf{c}_{1,2}, \mathbf{c}_{1,3}, \dots, \mathbf{c}_{1,k^*}, \dots, \mathbf{c}_{k^*-1,k^*}\}$ .  $\Pi_i$  denotes the parents of  $v_i \in V_{\mathbf{G}}$  and  $\widehat{\Pi}_i = \prod_{v_j \in \Pi_i} \widehat{v}_j$ , where  $\widehat{v}_j$  is the number of categories of  $v_j$ . In particular, we have

$$\widehat{v}_j = \begin{cases} \ell & \text{if } v_j \in V_{\mathbf{t}}, \\ M+1 & \text{if } v_j \in V_{\mathbf{a}}, \\ 8 & \text{if } v_j \in V_{\mathbf{r}}, \\ c_j & \text{if } v_j \in V_{\mathbf{c}}. \end{cases}$$

where  $c_j$  is a constant. Suppose the corresponding variable  $\mathbf{c}_{n',n}$  of the node  $v_j \in V_{\mathbf{c}}$  equals  $|C_z|$ , we have

$$c_j = \begin{cases} 1 & \text{if } 1 \leq z \leq 7, \\ 3 & \text{if } z = 8 \text{ or } 9, \\ 5 & \text{if } z = 10, \\ 7 & \text{if } z = 11. \end{cases}$$

Since the structure between  $\mathbf{t}$  and  $\mathbf{a}$ , the structure among  $\mathbf{t}$  and the structure between  $\mathbf{c}$  and  $\mathbf{r}$  are fixed, the number of parents of a node  $v_i \in V_{\mathbf{t}} \cup V_{\mathbf{a}} \cup V_{\mathbf{c}}$  are fixed. Then, we have

$$\widehat{\Pi}_i = \begin{cases} \ell^{i-1} & \text{if } v_i \in V_{\mathbf{t}}, \\ \ell & \text{if } v_i \in V_{\mathbf{a}}, \\ 1 & \text{if } v_i \in V_{\mathbf{c}}. \end{cases}$$

Also, let  $\Phi$  be the entire vector of parameters such that  $\forall_{ijk} : \phi_{ijk} = P(v_{ik} | \pi_{ij})$ , where  $v_{ik}$  and  $\pi_{ij}$  denotes that  $v_i$  is assigned with the  $k$ -th element and its parent is assigned with the  $j$ -th element in  $\widehat{\Pi}_i$ , respectively;  $n_{ijk}$  indicates how many

instances of  $\mathbb{D}$  contain both  $v_{ik}$  and  $\pi_{ij}$ . Here, we split the parameter vector  $\Phi$  into three parts:  $\Phi^{(1)}$ ,  $\Phi^{(2)}$ ,  $\Phi^{(0)}$  and  $\Phi^{(3)}$  are the parameter vectors associated with  $V_{\mathbf{t}}$ ,  $V_{\mathbf{a}}$ ,  $V_{\mathbf{r}}$  and  $V_{\mathbf{c}}$ , respectively. Given a training dataset  $\mathbb{D}_l$ , we have

$$\begin{aligned} \text{BIC-Score}(\mathbf{G} : \mathbb{D}_l) &= \max_{\Phi} L_{\mathbf{G}, \mathbb{D}_l}(\Phi) - \frac{\log|\mathbb{D}_l|}{2} \cdot |\Phi| \\ &= \max_{\Phi} \log \prod_{i=1}^{V_{\mathbf{G}}} \prod_{j=1}^{\widehat{\Pi}_i} \prod_{k=1}^{\widehat{v}_i} \phi_{ijk}^{n_{ijk}} - \frac{\log|\mathbb{D}_l|}{2} \cdot \sum_{i=1}^{V_{\mathbf{G}}} \widehat{\Pi}_i \cdot (\widehat{v}_i - 1) \\ &= \max_{\Phi} (\log \prod_{v_i \in V_{\mathbf{t}}} \prod_{j=1}^{\widehat{\Pi}_i} \prod_{k=1}^{\widehat{v}_i} \phi_{ijk}^{n_{ijk}} + \log \prod_{v_i \in V_{\mathbf{a}}} \prod_{j=1}^{\widehat{\Pi}_i} \prod_{k=1}^{\widehat{v}_i} \phi_{ijk}^{n_{ijk}} + \log \prod_{v_i \in V_{\mathbf{r}}} \prod_{j=1}^{\widehat{\Pi}_i} \prod_{k=1}^{\widehat{v}_i} \phi_{ijk}^{n_{ijk}} + \log \prod_{v_i \in V_{\mathbf{c}}} \prod_{j=1}^{\widehat{\Pi}_i} \prod_{k=1}^{\widehat{v}_i} \phi_{ijk}^{n_{ijk}}) \\ &\quad - \frac{\log|\mathbb{D}_l|}{2} \cdot (\sum_{v_i \in V_{\mathbf{t}}} \widehat{\Pi}_i \cdot (\widehat{v}_i - 1) + \sum_{v_i \in V_{\mathbf{a}}} \widehat{\Pi}_i \cdot (\widehat{v}_i - 1) + \sum_{v_i \in V_{\mathbf{r}}} \widehat{\Pi}_i \cdot (\widehat{v}_i - 1) + \sum_{v_i \in V_{\mathbf{c}}} \widehat{\Pi}_i \cdot (\widehat{v}_i - 1)) \\ &= \max_{\Phi^{(1)}} \log \prod_{i=1}^{k^*} \prod_{j=1}^{\ell-1} \prod_{k=1}^{\ell} (\phi_{ijk}^{(1)})^{n_{ijk}} - \frac{\log|\mathbb{D}_l|}{2} \cdot k^* \cdot \ell^{i-1} \cdot (\ell - 1) \\ &\quad + \max_{\Phi^{(2)}} \log \prod_{i=1}^{k^*} \prod_{j=1}^{\ell} \prod_{k=1}^{M+1} (\phi_{ijk}^{(2)})^{n_{ijk}} - \frac{\log|\mathbb{D}_l|}{2} \cdot k^* \cdot \ell \cdot M \\ &\quad + \max_{\Phi^{(3)}} \log \prod_{i=1}^{k^*(k^*-1)/2} \prod_{j=1}^1 \prod_{k=1}^{c_i} (\phi_{ijk}^{(3)})^{n_{ijk}} - \frac{\log|\mathbb{D}_l|}{2} \cdot \sum_{i=1}^{k^*(k^*-1)/2} (c_i - 1) \\ &\quad + \max_{\Phi^{(0)}} \log \prod_{v_i \in V_{\mathbf{r}}} \prod_{j=1}^8 (\phi_{ijk}^{(0)})^{n_{ijk}} - \frac{\log|\mathbb{D}_l|}{2} \cdot \frac{k^*(k^*-1)}{2} \cdot 7 \quad \triangleright \text{for } v_i \in V_{\mathbf{r}} \text{ and } \Pi_i \subset V_{\mathbf{c}} \\ &\quad + \max_{\Phi^{(0)}} \log \prod_{v_i \in V_{\mathbf{r}}} \prod_{j=1}^8 (\phi_{ijk}^{(0)})^{n_{ijk}} - \frac{\log|\mathbb{D}_l|}{2} \cdot \sum_{v_i \in V_{\mathbf{r}}} \widehat{\Pi}_i \cdot 7 \quad \triangleright \text{for } v_i \in V_{\mathbf{r}} \text{ and } \Pi_i \subset V_{\mathbf{a}}. \end{aligned}$$

Similarly, in  $\mathbf{G}'$ , any node  $v_i \in U_{\mathbf{G}'}$  has no parent, and thus  $\widehat{\Pi}_i = 1$ . We split the parameter vector  $\Phi$  into two parts:  $\Phi^{(4)}$  and  $\Phi^{(0)}$  are the parameter vectors associated with  $U_{\mathbf{G}'}$  and  $W_{\mathbf{G}'}$ , respectively. Then, we have

$$\begin{aligned} \text{BIC-Score}(\mathbf{G}' : \mathbb{D}_l) &= \max_{\Phi} L_{\mathbf{G}', \mathbb{D}_l}(\Phi) - \frac{\log|\mathbb{D}_l|}{2} \cdot |\Phi| \\ &= \max_{\Phi} \log \prod_{i=1}^{V_{\mathbf{G}'}} \prod_{j=1}^{\widehat{\Pi}_i} \prod_{k=1}^{\widehat{v}_i} \phi_{ijk}^{n_{ijk}} - \frac{\log|\mathbb{D}_l|}{2} \cdot \sum_{i=1}^{V_{\mathbf{G}'}} \widehat{\Pi}_i \cdot (\widehat{v}_i - 1) \\ &= \max_{\Phi^{(4)}} \log \prod_{i=1}^{k^*} \prod_{j=1}^1 \prod_{k=1}^{M+1} (\phi_{ijk}^{(4)})^{n_{ijk}} - \frac{\log|\mathbb{D}_l|}{2} \cdot k^* \cdot M \\ &\quad + \max_{\Phi^{(0)}} \log \prod_{v_i \in W_{\mathbf{G}'}} \prod_{j=1}^8 (\phi_{ijk}^{(0)})^{n_{ijk}} - \frac{\log|\mathbb{D}_l|}{2} \cdot \sum_{v_i \in W_{\mathbf{G}'}} \widehat{\Pi}_i \cdot 7. \end{aligned}$$

Let

$$\begin{aligned} \lambda &= (\max_{\Phi^{(1)}} \log \prod_{i=1}^{k^*} \prod_{j=1}^{\ell-1} \prod_{k=1}^{\ell} (\phi_{ijk}^{(1)})^{n_{ijk}} - \frac{\log|\mathbb{D}_l|}{2} \cdot k^* \cdot \ell^{i-1} \cdot (\ell - 1)) \\ &\quad + (\max_{\Phi^{(2)}} \log \prod_{i=1}^{k^*} \prod_{j=1}^{\ell} \prod_{k=1}^{M+1} (\phi_{ijk}^{(2)})^{n_{ijk}} - \frac{\log|\mathbb{D}_l|}{2} \cdot k^* \cdot \ell \cdot M) \\ &\quad + (\max_{\Phi^{(3)}} \log \prod_{i=1}^{k^*(k^*-1)/2} \prod_{j=1}^1 \prod_{k=1}^{c_i} (\phi_{ijk}^{(3)})^{n_{ijk}} - \frac{\log|\mathbb{D}_l|}{2} \cdot \sum_{i=1}^{k^*(k^*-1)/2} (c_i - 1)) \\ &\quad + (\max_{\Phi^{(0)}} \log \prod_{v_i \in V_{\mathbf{r}}} \prod_{j=1}^8 (\phi_{ijk}^{(0)})^{n_{ijk}} - \frac{\log|\mathbb{D}_l|}{2} \cdot \frac{k^*(k^*-1)}{2} \cdot 7) \quad \triangleright \text{for } v_i \in V_{\mathbf{r}} \text{ and } \Pi_i \subset V_{\mathbf{c}} \\ &\quad - (\max_{\Phi^{(4)}} \log \prod_{i=1}^{k^*} \prod_{j=1}^1 \prod_{k=1}^{M+1} (\phi_{ijk}^{(4)})^{n_{ijk}} - \frac{\log|\mathbb{D}_l|}{2} \cdot k^* \cdot M). \end{aligned}$$

Given a dataset  $\mathbb{D}_l$ , the parameter vectors  $\Phi^{(1)}$ ,  $\Phi^{(2)}$ ,  $\Phi^{(3)}$ ,  $\Phi^{(4)}$  can be estimated to maximize their respective logarithmic equations regardless of the network structures. Similarly, for the parameters  $\phi_{ijk}^{(0)} \in \Phi^{(0)}$  such that  $v_i \in V_{\mathbf{r}}$  and  $\Pi_i \subset V_{\mathbf{c}}$ , they can also be estimated invariantly under arbitrary network structures. Therefore,  $\lambda$  is constant. Then we have

$$\text{BIC-Score}(\mathbf{G} : \mathbb{D}_l) = \text{BIC-Score}(\mathbf{G}' : \mathbb{D}_l) + \lambda.$$

□

## APPENDIX C

## CONDITIONAL DISTRIBUTION FOR GIBBS SAMPLING

Since the probability of  $\mathbf{a}_n$  conditioned on  $\mathbf{t}_n$  is Dirichlet-multinomial distribution, we can write out the integration formulae:

$$\begin{aligned} \prod_{d=1}^{|d|} \prod_{n=1}^{\ell} P(\mathbf{a}_n | \mathbf{t}_n; \beta) &= \prod_{k=1}^{\ell} P(\mathbf{a} | T_k; \beta) = \prod_{k=1}^{\ell} \int_{\theta_k} P(\mathbf{a} | \theta_k) P(\theta_k; \beta) d\theta_k \\ &= \prod_{k=1}^{\ell} \frac{\Gamma(\sum_{i'=1}^M \beta_{k,i'})}{\Gamma(\sum_{i'=1}^M (na_{k,i'} + \beta_{k,i'}))} \prod_{i'=1}^M \frac{\Gamma(na_{k,i'} + \beta_{k,i'})}{\Gamma(\beta_{k,i'})} \end{aligned}$$

The total number of tables cannot exceed the maximum network size  $\ell$ .

The probability of  $\mathbf{t}_n$  conditioned on its previous tables  $\mathbf{t}_1, \mathbf{t}_2, \dots, \mathbf{t}_{n-1}$  follows CRP ( $n \geq 2$ ). We adopt the technique introduced by Sudderth [27] to sample the  $n$ -th table in  $G_d$  as follows

$$P(\mathbf{t}_n = T_\zeta | \mathbf{t}_1, \mathbf{t}_2, \dots, \mathbf{t}_{n-1}; \alpha_\zeta) = \frac{1}{n + \alpha_\zeta - 1} \left( \sum_{k=1}^{NT_n} nt_k \delta(\zeta, k) + \alpha_\zeta \delta(\zeta, \bar{k}) \right)$$

where  $nt_k$  is the number of time the previous  $n-1$  nodes in  $G_d$  are assigned to the table  $T_k$ , and  $\delta$  is the Kronecker delta function that

$$\delta(\zeta, k) = \begin{cases} 1 & \text{if } \zeta = k \\ 0 & \text{if } \zeta \neq k \end{cases}$$

and  $\bar{k}$  denotes a previously empty table.

Now we derive the conditional probability of each variable  $\mathbf{t}_n$  of the  $n$ -th table in  $G_d$  assigned to the table  $T_\zeta$  by Gibbs sampling as follows:

$$\begin{aligned} P(\mathbf{t}_n = T_\zeta | \mathbf{t}_{-n}, \mathbf{a}, \mathbf{r}; \alpha, \beta) &\propto P(\mathbf{t}_n, \mathbf{t}_{-n}, \mathbf{a}, \mathbf{r}; \alpha, \beta) \\ &= \prod_{d=1}^{|d|} \prod_{n=1}^{\ell} P(\mathbf{a}_n | \mathbf{t}_n; \beta) \times \prod_{d=2}^{|d|} \prod_{n=2}^{\ell} P(\mathbf{t}_n | \mathbf{t}_1, \dots, \mathbf{t}_{n-1}; \alpha) \times \prod_{d=2}^{|d|} \prod_{n=2}^{\ell} P(\mathbf{r}_{n-1,n} | \mathbf{a}_{n-1}, \mathbf{a}_n) \\ &\propto \prod_{d=1}^{|d|} \prod_{n=1}^{\ell} P(\mathbf{a}_n | \mathbf{t}_n; \beta) \times P(\mathbf{t}_n | \mathbf{t}_1, \dots, \mathbf{t}_{n-1}; \alpha) \times \prod_{n \neq \mathbf{n}} P(\mathbf{t}_n | \mathbf{t}_1, \dots, \mathbf{t}_{n-1}; \alpha) \\ &\times \prod_{d \neq \mathbf{d}} \prod_{n=2}^{\ell} P(\mathbf{t}_n | \mathbf{t}_1, \dots, \mathbf{t}_{n-1}; \alpha) \\ &\propto \prod_{k=1}^{\ell} \frac{\Gamma(\sum_{i'=1}^M \beta_{k,i'})}{\Gamma(\sum_{i'=1}^M (na_{k,i'} + \beta_{k,i'}))} \prod_{i=1}^M \frac{\Gamma(na_{k,i} + \beta_{k,i})}{\Gamma(\beta_{k,i})} \times \frac{1}{n + \alpha_\zeta - 1} \left( \sum_{k=1}^{NT_n} nt_k \delta(\zeta, k) + \alpha_\zeta \delta(\zeta, \bar{k}) \right) \\ &\propto \frac{\prod_{i=1}^M \Gamma(na_{\zeta,i} + \beta_{\zeta,i})}{\Gamma(\sum_{i'=1}^M (na_{\zeta,i'} + \beta_{\zeta,i'}))} \prod_{k \neq \zeta} \frac{\prod_{i=1}^M \Gamma(na_{k,i} + \beta_{k,i})}{\Gamma(\sum_{i'=1}^M (na_{k,i'} + \beta_{k,i'}))} \\ &\times \frac{1}{n + \alpha_\zeta - 1} \left( \sum_{k=1}^{NT_n} nt_k \delta(\zeta, k) + \alpha_\zeta \delta(\zeta, \bar{k}) \right) \\ &\propto \frac{\Gamma(na_{\zeta,i,-n} + \beta_{\zeta,i} + 1) \prod_{i \neq \bar{i}} \Gamma(na_{\zeta,i,-n} + \beta_{\zeta,i})}{\Gamma(\sum_{i'=1}^M (na_{\zeta,i',-n} + \beta_{\zeta,i'} + 1))} \prod_{k \neq \zeta} \frac{\prod_{i=1}^M \Gamma(na_{k,i,-n} + \beta_{k,i})}{\Gamma(\sum_{i'=1}^M (na_{k,i',-n} + \beta_{k,i'}))} \\ &\times \frac{1}{n + \alpha_\zeta - 1} \left( \sum_{k=1}^{NT_n} nt_k \delta(\zeta, k) + \alpha_\zeta \delta(\zeta, \bar{k}) \right) \\ &= \frac{na_{\zeta,i,-n} + \beta_{\zeta,i}}{\sum_{i'=1}^M (na_{\zeta,i',-n} + \beta_{\zeta,i'})} \prod_{k=1}^{\ell} \frac{\prod_{i=1}^M \Gamma(na_{k,i,-n} + \beta_{k,i})}{\Gamma(\sum_{i'=1}^M (na_{k,i',-n} + \beta_{k,i'}))} \\ &\times \frac{1}{n + \alpha_\zeta - 1} \left( \sum_{k=1}^{NT_n} nt_k \delta(\zeta, k) + \alpha_\zeta \delta(\zeta, \bar{k}) \right) \\ &\propto \frac{na_{\zeta,i,-n} + \beta_{\zeta,i}}{\sum_{i'=1}^M (na_{\zeta,i',-n} + \beta_{\zeta,i'})} \times \frac{1}{n + \alpha_\zeta - 1} \left( \sum_{k=1}^{NT_n} nt_k \delta(\zeta, k) + \alpha_\zeta \delta(\zeta, \bar{k}) \right) \\ &= \begin{cases} \frac{na_{\zeta,i,-n} + \beta_{\zeta,i}}{\sum_{i'=1}^M (na_{\zeta,i',-n} + \beta_{\zeta,i'})} \times \frac{nt_\zeta}{n + \alpha_\zeta - 1} & \text{if } \zeta \leq NT_n \\ \frac{na_{\zeta,i,-n} + \beta_{\zeta,i}}{\sum_{i'=1}^M (na_{\zeta,i',-n} + \beta_{\zeta,i'})} \times \frac{\alpha_\zeta}{n + \alpha_\zeta - 1} & \text{if } \zeta = NT_n + 1 \end{cases} \end{aligned}$$

## REFERENCES

[1] Aggarwal, J., Ryooy, M.: Human activity analysis: A review. *ACM Computing Surveys* **43**(3), 16 (2011)

[2] Allen, J.: Maintaining knowledge about temporal intervals. *ACM Communications* **26**(11), 832–843 (1983)

[3] Brendel, W., Fern, A., Todorovic, S.: Probabilistic event logic for interval-based event recognition. In: *CVPR* (2011)

[4] Bulling, A., Blanke, U., Schiele, B.: A tutorial on human activity recognition using body-worn inertial sensors. *ACM Computing Surveys* **46**(3), 33 (2014)

[5] Campos, C.D., Ji, Q.: Efficient structure learning of Bayesian networks using constraints. *JMLR* **12**, 663–689 (2011)

[6] Chen, L., Hoey, J., Nugent, C., Cook, D., Yu, Z.: Sensor-based activity recognition. *Systems, Man, and Cybernetics, Part C: Applications and Reviews, IEEE Transactions on* **42**(6), 790–808 (2012)

[7] Cook, D.J., Krishnan, N.C., Rashidi, P.: Activity discovery and activity recognition: a new partnership. *IEEE Transactions on Cybernetics* **43**(3), 820–828 (2013)

[8] Devanne, M., Wannous, H., Berretti, S., Pala, P.: 3-d human action recognition by shape analysis of motion trajectories on riemannian manifold. *IEEE Transactions on Cybernetics* **45**(7), 1023–1029 (2014)

[9] Dubba, K.S.R., Cohn, A.G., Hogg, D.C., Bhatt, M., Dylla, F.: Learning relational event models from video. *Journal of Artificial Intelligence Research* **53**(1), 41–90 (2015)

[10] Fan, X., Yuan, C.: An improved lower bound for Bayesian network structure learning. In: *AAAI* (2015)

[11] Helaoui, R., Niepert, M., Stuckenschmidt, H.: Recognizing interleaved and concurrent activities: A statistical-relational approach. In: *IEEE International Conference on Pervasive Computing and Communications* (2011)

[12] Hu, D., Yang, Q.: CIGAR: Concurrent and interleaving goal and activity recognition. In: *AAAI* (2008)

[13] Kim, E., Helal, S., Cook, D.: Human activity recognition and pattern discovery. *IEEE Pervasive Computing* **9**(1), 48–53 (2010)

[14] Lara, O.D., Labrador, M.: A survey on human activity recognition using wearable sensors. *IEEE Communications Surveys & Tutorials* **15**(3), 1192–1209 (2013)

[15] Lillo, I., Soto, A., Niebles, J.: Discriminative hierarchical modeling of spatio-temporally composable human activities. In: *CVPR* (2014)

[16] Liu, A.A., Su, Y.T., Jia, P.P., Gao, Z., Hao, T., Yang, Z.X.: Multiple/single-view human action recognition via part-induced multitask structural learning. *IEEE Transactions on Cybernetics* **45**(6), 1194–1208 (2015)

[17] Liu, L., Cheng, L., Liu, Y., Jia, Y., Rosenblum, D.: Recognizing complex activities by a probabilistic interval-based model. In: *AAAI* (2016)

[18] Liu, L., Wang, S., Peng, Y., Huang, Z., Liu, M., Hu, B.: Mining intricate temporal rules for recognizing complex activities of daily living under uncertainty. *Pattern Recognition* **60**, 1015–1028 (2016)

[19] Minka, T.: Estimating a Dirichlet distribution (2000)

[20] Modayil, J., Bai, T., Kautz, H.: Improving the recognition of interleaved activities. In: *Int. Conf. Ubiquitous computing* (2008)

[21] Oliver, N., Horvitz, E.: A comparison of hmms and dynamic Bayesian networks for recognizing office activities. In: *User Modeling*, pp. 199–209 (2005)

[22] Pinhanez, C.S.: Representation and recognition of action in interactive spaces. Ph.D. thesis, MIT (1999)

[23] Pitman, J.: Combinatorial stochastic processes. Tech. rep., Technical Report 621, Dept. Statistics, UC Berkeley (2002)

[24] Raftery, A.E., Lewis, S.: How many iterations in the Gibbs sampler. *Bayesian statistics* **4**(2), 763–773 (1992)

[25] Roggen, D., Calatroni, A., Rossi, M., Holleczeck, T., et al.: Collecting complex activity datasets in highly rich networked sensor environments. In: *Int. Conf. Networked Sensing Systems* (2010)

[26] Ryooy, M., Aggarwal, J.: Semantic representation and recognition of continued and recursive human activities. *Int. j. of compt. vision* **82**(1), 1–24 (2009)

[27] Sudderth, E.B.: Graphical models for visual object recognition and tracking. Ph.D. thesis, MIT (2006)

[28] Teh, Y.W.: Dirichlet process. In: *Encyclopedia of machine learning*, pp. 280–287 (2011)

[29] Veeraraghavan, H., Papanikolopoulos, N., Schrater, P.: Learning dynamic event descriptions in image sequences. In: *IEEE Conference on Computer Vision & Pattern Recognition*, pp. 1–6 (2007)

[30] Xu, C., Nanjappa, A., Zhang, X., Cheng, L.: Estimate hand poses efficiently from single depth images. *International Journal of Computer Vision* **116**(1), 21–45 (2016)

[31] Zhang, Y., Zhang, Y., Swears, E., Larios, N., Wang, Z., Ji, Q.: Modeling temporal interactions with interval temporal Bayesian networks for complex activity recognition. *IEEE Transactions on Pattern Analysis and Machine Intelligence* **35**(10), 2468–2483 (2013)